

# Transport Systems of *Ventricaria ventricosa*: Asymmetry of the Hyper- and Hypotonic Regulation Mechanisms

M. A. Bisson · M. J. Beilby

Received: 6 June 2008 / Accepted: 17 September 2008  
© Springer Science+Business Media, LLC 2008

**Abstract** Hyper- and hypotonic stresses elicit apparently symmetrical responses in the alga *Ventricaria*. With hypertonic stress, membrane potential difference (PD) between the vacuole and the external medium becomes more positive, conductance at positive PDs ( $G_m^{\text{pos}}$ ) increases and KCl is actively taken up to increase turgor. With hypotonic stress, the membrane PD becomes more negative, conductance at negative PDs ( $G_m^{\text{neg}}$ ) increases and KCl is lost to decrease turgor. We used inhibitors that affect active transport to determine whether agents that inhibit the  $K^+$  pump and hypertonic regulation also inhibit hypotonic regulatory responses. Cells whose turgor pressure was held low by the pressure probe (turgor-clamped) exhibited the same response as cells challenged by hyperosmotic medium, although the response was maintained longer than in osmotically challenged cells, which regulate turgor. The role of active  $K^+$  transport was confirmed by the effects of decreased light, dichlorophenyldimethyl urea and diethylstilbestrol, which induced a uniformly low conductance (quiet state). Cells clamped to high turgor exhibited the same response as cells challenged by hypo-osmotic medium, but the response was similarly transient, making effects of inhibitors hard to determine. Unlike clamped cells, cells challenged by hypo-osmotic medium responded to inhibitors with rapid, transient, negative-going PDs, with

decreased  $G_m^{\text{neg}}$  and increased  $G_m^{\text{pos}}$  (linearized  $I-V$ ), achieving the quiet state as PD recovered. These changes are different from those exerted on the pump state, indicating that different transport systems are responsible for turgor regulation in the two cases.

**Keywords** *Ventricaria (Valonia)* · Turgor clamp · Light effect · Dichlorophenyldimethyl urea · Diethylstilbestrol ·  $I-V$  characteristics · Hypotonic regulation · Hypertonic regulation

## Introduction

*Valonia* and its sister genus *Ventricaria* have long been objects of study for their transport properties, particularly the response of transport systems to osmotic stress required to regulate turgor (Osterhout 1924; Damon 1930; Kopak 1933; Bisson et al. 2006). Their structure and electrophysiological properties are strikingly different from many other plant and algal cells (see Bisson et al. 2006, and Shepherd et al. 2004, for recent reviews). Under control conditions, the electrical potential difference (PD) across the two membranes, plasma membrane and tonoplast, is small and positive (with respect to the external medium), reportedly due to similar (but opposite) membrane potentials at each membrane (Damon 1930; Davis 1981). The conductance is similar at the two membranes, so the changes in overall conductance cannot be attributed primarily to the plasma membrane as in many plants (Bisson et al. 2006). In the response to hypertonic stress (decrease in turgor due to increase in external osmotic pressure), the PD becomes more positive, and this has been unambiguously associated with an increase of active uptake of  $K^+$  at the tonoplast, with accompanying  $Cl^-$  uptake that may be active or

---

M. A. Bisson (✉)  
Department of Biological Sciences, State University of New York at Buffalo, Cooke Hall 109, Buffalo, NY 14260-1300, USA  
e-mail: bisson@acsu.buffalo.edu

M. J. Beilby  
Biophysics, School of Physics, University of New South Wales, Sydney 2052, Australia  
e-mail: mjb@newt.phys.unsw.edu.au

passive. This results in accumulation of KCl in the vacuole, increase of internal osmotic pressure and restoration of turgor.  $I$ - $V$  analysis has shown that this is associated with an increase in conductance at positive potentials ( $G_m^{\text{pos}}$ ) (Beilby and Bisson 1999; Bisson and Beilby 2002). Many questions remain unresolved, including the nature of the response to hypotonic stress (increased turgor due to decreased external osmotic pressure). The cell must lose KCl to restore normal turgor, but whether this is done passively or actively is not clear. Hypotonic regulation is associated with a more negative PD and an increase in conductance at negative potentials ( $G_m^{\text{neg}}$ ). This could be due to an increase in passive  $K^+$  conductance at the tonoplast or an outwardly directed pump at the plasma membrane.

We utilized light and inhibitors to discriminate between these possibilities. We employed turgor clamping to separate water stress from changes in ion composition of the medium, as well as ambiguities that arise from turgor regulation during the experiment. The  $I$ - $V$  curve technique was used to monitor the electrical characteristics of the membrane transporters (Beilby 1990).

## Materials and Methods

### Cell Culture

*Ventricaria ventricosa* was initially collected on Heron Island, off Queensland, Australia, and subsequently cultured in natural or artificial seawater (ASW) as described previously (Bisson and Beilby 2002). The cells were grown under low-intensity white light, about  $0.35 \mu\text{mol s}^{-1} \text{m}^{-2}$ . The experiments were performed on cells with a diameter of 2.0–2.5 mm.

### Media and Conditions

During the experiments, cells were bathed in simplified ASW composed of (in mM) 450 NaCl, 10 KCl, 50  $\text{MgSO}_4$ , 8  $\text{CaCl}_2$ , buffered to pH 8.0 with 10 HEPES (4-2[hydroxyethyl]-1-piperazine-ethane sulfonic acid) and NaOH, osmotic pressure of 990 mOsm  $\text{kg}^{-1}$ . The osmolarity was measured by a cryoscopic osmometer (Osmomat 030; Gally Scientific, North Melbourne, Australia). To lower the osmotic pressure of ASW from 990 to 790 mOsm  $\text{kg}^{-1}$ , the NaCl concentration was decreased.

Diethylstilbestrol (DES) was dissolved in 1% methanol and dichlorophenyldimethyl urea (DCMU) in 1% ethanol in at least  $10\times$  concentration. The 0.1% methanol and 0.1% ethanol controls had no effect on membrane PD,  $I$ - $V$  characteristics or turgor of the cells.

Cell illumination was provided by a fiber-optic light source and could be varied from light off ( $0.5 \mu\text{mol s}^{-1} \text{m}^{-2}$ )

to bright light ( $40 \mu\text{mol s}^{-1} \text{m}^{-2}$ ). The light intensity was measured by a quantum photometer (LI-250; LI-COR, Lincoln, NE).

### Electrophysiological Measurements

Cells were impaled and voltage-clamped by the two-electrode technique, and  $I$ - $V$  curves were obtained as described previously (Beilby and Bisson 1999). As the double impalement by the current-injecting electrode and the pressure probe resulted in long recovery times (Bisson and Beilby 2002), the current-injecting electrode was made smaller. We used much thinner Pt/Ir wire of 0.005 mm diameter (Goodfellow, Oakdale, PA). This wire was too thin to penetrate the tough *Ventricaria* wall. The wire was threaded through the microelectrode glass, which was then pulled into two electrodes in the horizontal puller (model P-87; Sutter Instrument, Novato, CA). The electrodes had narrow tips of  $<10 \mu\text{m}$ , with the glass melted on the wire. The wire tip was left protruding about 1 mm and bent back so that the glass could be used to penetrate the wall. The electrode tip was positioned in the middle of the cell. This electrode delivered all the necessary clamp current and was less damaging to the cells.

The cells were clamped to a bipolar staircase protocol generated by LSI 11/73 computer with pulses of 100 ms separated by 250 ms at the resting membrane PD level. The last 10 points of each membrane PD and current staircase pulse were averaged to form the  $I$ - $V$  profile. The data logging of each  $I$ - $V$  profile took 8 s. Polynomials were fitted to the  $I$ - $V$  data using Mathematica 5.2 (Wolfram Research, Champaign, IL). Initially, each data set was fitted by a single polynomial; but if the fit was not satisfactory, the procedure was repeated for data segments, three points at a time.

### Turgor Measurement and Control

To measure and control turgor pressure, cells were impaled with a turgor probe, as described previously (Bisson and Beilby 2002). Briefly, the tip of a glass micropipette was beveled at 45 degrees to obtain a sharp point and an opening of about  $50 \mu\text{m}$  diameter. The micropipettes were then filled with silicone oil and connected to a pressure transducer. The volume of the micropipette could be controlled by manually moving a piston in the probe. To measure turgor, the meniscus between the silicone oil and the aqueous cell sap was maintained at a predetermined point. The probe was also utilized to control turgor (turgor clamp) (Wendler and Zimmermann 1982; Zhu and Boyer 1992; Heidecker et al. 2003). In this case a sacrificial cell was impaled and sap was withdrawn to fill the micropipette. This cell was discarded, and an experiment was

performed on a new cell. Turgor was manipulated by injecting or withdrawing sap and could be maintained at a steady level for over 1 h. The range extended from zero turgor to about 0.3 MPa. Above that value, seals could not be maintained reliably. The meniscus had to be constantly manipulated to keep the turgor at the desired level. Some elevated turgor experiments were terminated when all the cell sap in the pipette had been injected. While the cells could tolerate injection of a small amount of silicone oil, excess silicone oil was damaging.

## Results

### Unstressed Cells: Effects of Light and Inhibitors

In photosynthetic cells, changes in light may change the availability of energy sources to active transport systems. We therefore examined the effect of light on unstressed cells. Figure 1 illustrates a typical response of the  $I$ - $V$  characteristics to light. In dim light of  $9.5 \mu\text{mol s}^{-1} \text{m}^{-2}$

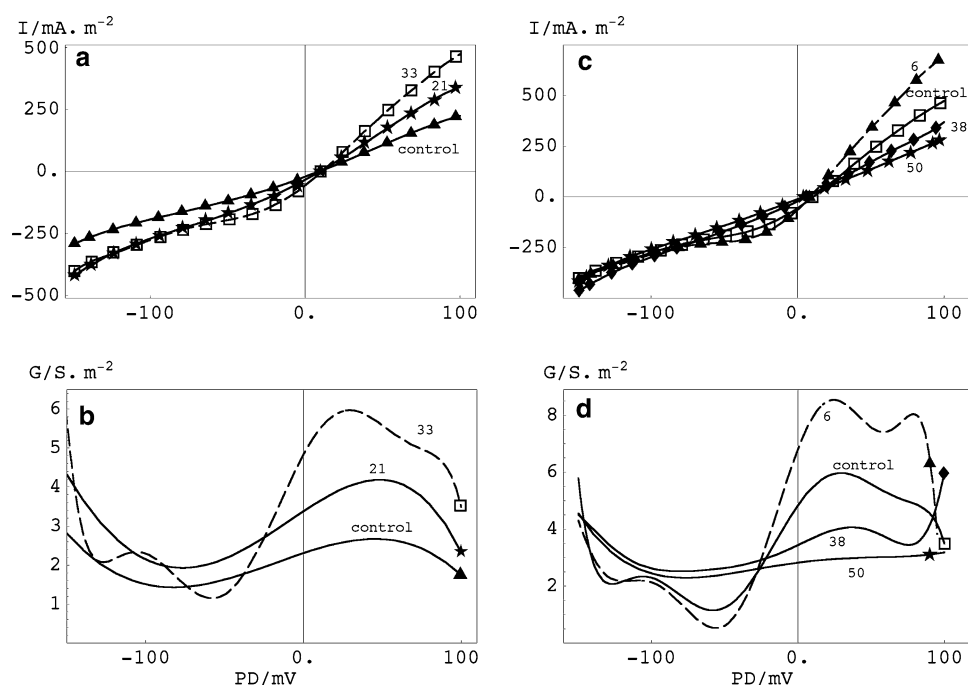


**Fig. 1** A typical response to changes in light intensity. **a, b** Response to an increase in light intensity. The cell was impaled and reached steady state in dim light ( $9.5 \mu\text{mol s}^{-1} \text{m}^{-2}$ ) for about 4 h. The light intensity was then increased in step fashion to  $40.0 \mu\text{mol s}^{-1} \text{m}^{-2}$ . Line types are the same for both  $I$ - $V$  curves (**a**) and  $G$ - $V$  curves (**b**) with the symbols used in **a** attached to each relevant  $G$ - $V$  profile. The times (in min) after light intensity change are shown next to each curve. Control in dim light is shown by *filled triangles*. After 8 min in bright light the  $I$ - $V$  profile was almost identical to control (not shown). After 21 min of bright light the experimental points are depicted as *stars* and after 33 min as *empty squares* and *dashed line*.  $I$ - $V$  curve at 27 min of bright light was very similar to that at 33 min

the membrane potential was +10 mV and the conductance ( $G_m^{\text{pos}}$ ) was slightly higher in the positive range than in the negative ( $G_m^{\text{neg}}$ ) (Fig. 1a, b, triangles). Such a profile is typical of an unstressed cell that is maintaining its turgor but not regulating in response to osmotic stress (Bisson and Beilby 2002). When the light was increased to  $40 \mu\text{mol s}^{-1} \text{m}^{-2}$ , there was little effect on membrane potential. Initially, there was little change in conductance, but by 21 min  $G_m^{\text{pos}}$  started to increase. Maximum conductance was reached after 27 min (not shown) and maintained for at least 5 min (Fig. 1a, b, empty squares). At this point the microscope light was turned off. The room lights resulted in a dim illumination of  $0.23 \mu\text{mol s}^{-1} \text{m}^{-2}$  (Fig. 1c, d). Surprisingly, the initial response was a further increase in  $G_m^{\text{pos}}$ , which peaked about 6 min after the light decreased (Fig. 1c, d, triangles). Thereafter,  $G_m^{\text{pos}}$  decreased, reaching a level similar to that of the control after about 26 min. At 50 min the conductance profile between  $-110$  and  $+100$  mV became approximately linear, with the resting PD less positive at 6.9 mV (Fig. 1c, d, stars). Such a linear  $I$ - $V$  (and flat  $G$ - $V$ ) profile with resting

(not shown), indicating saturation. **c, d** Response to a decrease in light intensity. Once the  $I$ - $V$  profile had stabilized in bright light ( $40.0 \mu\text{mol s}^{-1} \text{m}^{-2}$ ), the light was turned off (total illumination  $0.23 \mu\text{mol s}^{-1} \text{m}^{-2}$ ). Line types are the same for both  $I$ - $V$  curves (**c**) and  $G$ - $V$  curves (**d**) with the symbols used in **c** attached to each relevant  $G$ - $V$  profile. The control in bright light (same curve as shown at 33 min in **a** and **b**) is depicted by *empty squares*, 6 min light off by *filled triangles* and *dashed line*, 38 min light off by *filled diamonds* and 50 min light off by *stars*. Note that conductance increased transiently after the light was turned off. Conductance dropped back to the control level by 26 min light off (not shown) and continued to decrease for 50 min

PD close to zero is regarded as inhibited, or quiet state. An average of three cells is shown in Fig. 4 (see below). The control cells at a light level of  $40 \mu\text{mol s}^{-1} \text{m}^{-2}$  (red line) show the characteristic “pumping” profile, with much higher  $G_m^{\text{pos}}$  at 100 mV than  $G_m^{\text{neg}}$  at  $-100$  mV. The average resting PD was  $+13.2$  mV (shown by the red diamond in Fig. 4b) and the average conductance was  $10 \text{ S m}^{-2}$ . Under dimmer light at levels of  $0.23\text{--}9.3 \mu\text{mol s}^{-1} \text{m}^{-2}$  (blue line), the conductance fell to an average of  $3.25 \text{ S m}^{-2}$ , while the PD was relatively unchanged at  $13.3$  mV (blue diamond in Fig. 4b). The difference between  $G_m^{\text{pos}}$  and  $G_m^{\text{neg}}$  was reduced.

If the response to decreased light is due to a decrease in energy available from photosynthesis, similar results would be predicted from addition of the photosynthesis inhibitor DCMU. Adding  $10 \mu\text{M}$  DCMU to cells in moderate light conditions (Fig. 2a, b) also resulted in a decrease in conductance, starting at 2 min (not shown), and a decrease in the ratio  $G_m^{\text{pos}}:G_m^{\text{neg}}$ . The response reached maximum at 20 min (Fig. 2a, b, stars). At this point, DCMU was washed out (Fig. 2c, d) and the original profile ( $G_m^{\text{pos}} > G_m^{\text{neg}}$ ) developed over the next 50 min (Fig. 2c, d, empty squares). The average of three cells treated with

DCMU is shown in Fig. 4 (green line). There is little difference between  $G_m^{\text{pos}}$  and  $G_m^{\text{neg}}$ , and the conductance at the resting PD of  $7.6$  mV was  $1.5 \text{ S m}^{-2}$  (green diamond).

DES is a well-known inhibitor of a number of transport ATPases. If it acts directly on the pump, rather than on an energy supply that would decay relatively slowly after inhibition of photosynthesis, it should act more rapidly. DES  $30 \mu\text{M}$  rapidly (within 6 min) decreased the high  $G_m^{\text{pos}}$  associated with active  $\text{K}^+$  uptake, from 10 to less than  $2 \text{ S m}^{-2}$ , with little change in PD (Fig. 3a, b, empty triangles). The effect of DES was slowly reversed with time, with initial recovery after 29 min of wash (not shown) and a strong increase in  $G_m^{\text{pos}}$  at 41 min (Fig. 3b, c, stars), although the conductance was still less than the control. In an average of eight  $I$ - $V$  curves from three cells (Fig. 4), the black line shows that  $G_m^{\text{pos}}$  at the resting PD of  $11.5$  mV (black diamond in Fig. 4b) decreased to  $1.1 \text{ S m}^{-2}$ .

#### Effect of Inhibitors on Hypo-Osmotic State

Since hypertonic stress exaggerates the “pump” state of the control, we predicted that the effect of inhibitors would be similar under control and hypertonic stress. We first

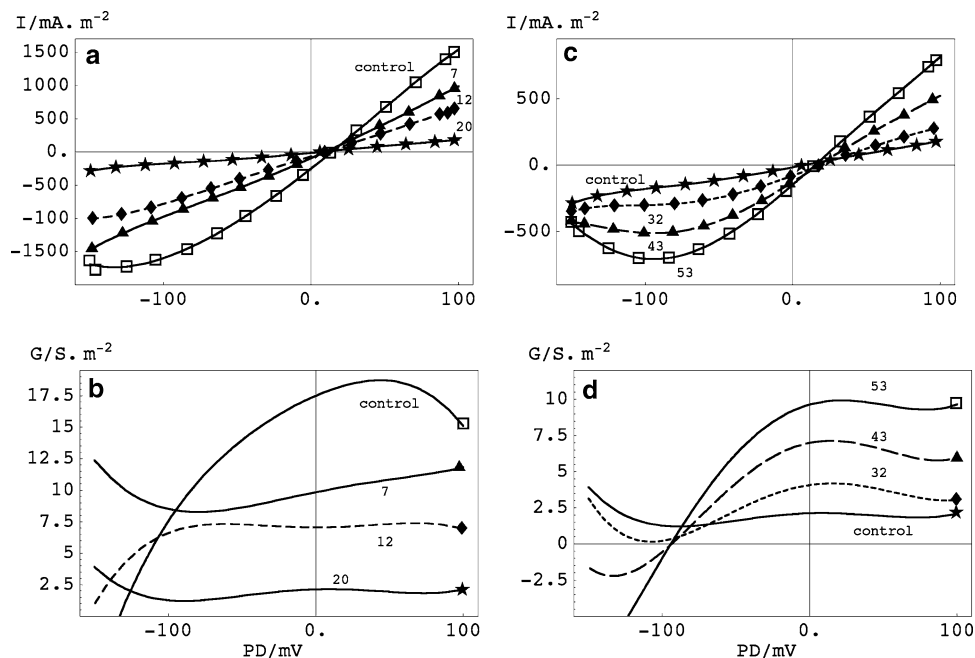


**Fig. 2** A typical response to  $10 \mu\text{M}$  DCMU. **a, b** Response to addition of DCMU. Symbols and line types are the same for both  $I$ - $V$  curves (**a**) and  $G$ - $V$  curves (**b**), with the symbols used in **a** attached to each relevant  $G$ - $V$  profile. The times (in min) after DCMU exposure are shown next to each curve. Control in ASW for 40 min is shown by empty squares. Exposure to DCMU: filled triangles at 7 min, similar to profile at 2 min (not shown), filled diamonds and dashed line at 12 min and much less conductive profile at 20 min, points depicted as stars. **c, d** Washout of DCMU. The wash sequence followed immediately after the inhibition sequence shown in **a** and **b**. Symbols

and line types are the same for both  $I$ - $V$  curves (**c**) and  $G$ - $V$  curves (**d**) with the symbols used in **c** attached to each relevant  $G$ - $V$  profile. The control was exposed to DCMU for 21 min and is shown by stars. The chamber was then washed out with ASW, but there was no change in the  $I$ - $V$  profile for 21 min (not shown). After 32 min the cell started to recover and the  $I$ - $V$  curve is shown with filled diamonds and short dashed line, after 43 min with filled triangles and long dashed line and finally after 53 min with empty squares. The cell did not recover to preexposure conductance but reached peak conductance of  $10 \text{ S m}^{-2}$

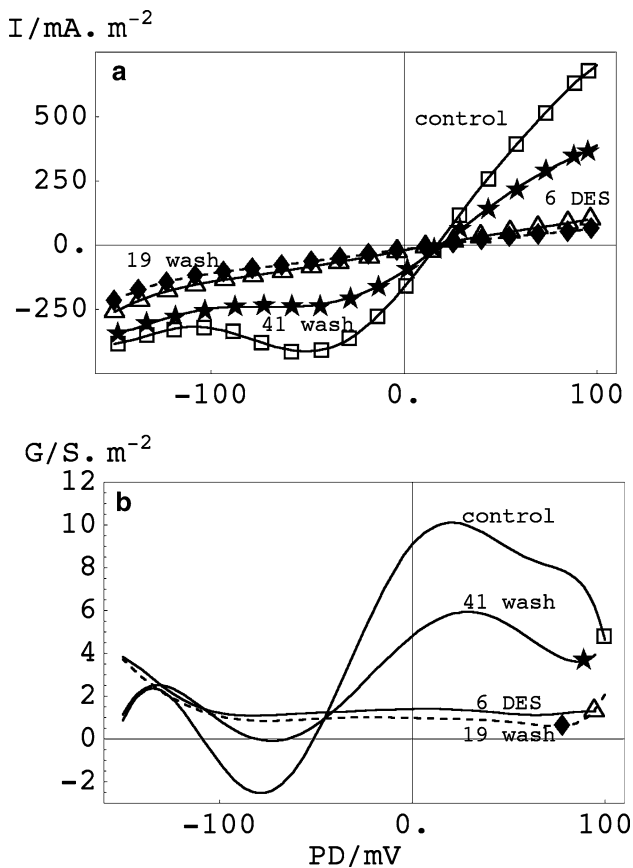


**Fig. 3** A typical response to  $30 \mu\text{M}$  DES and subsequent washout. Line types are the same for both  $I$ - $V$  curves (a) and  $G$ - $V$  curves (b) with the symbols used in a attached to each relevant  $G$ - $V$  profile. Control after 19 min in light of  $9.5 \mu\text{mol s}^{-1} \text{m}^{-2}$  is shown by *empty squares* and exhibits high conductance at positive PDs. Total inhibition, achieved 6 min after addition of DES, is shown by *empty triangles*. Recovery after the wash of DES was a more gradual process. A slight drop in conductance was seen after 5-min wash (not shown). After 19-min wash, the  $I$ - $V$  profile was unchanged and is shown as *filled diamonds* and *short dashed line*. After 41-min wash (*stars*), some recovery was seen

examined the effect of the rapidly acting DES on an osmotically stressed cell. The osmotic pressure of ASW (see “Materials and Methods”) was decreased from 990 to  $790 \text{ mOsmol kg}^{-1}$  by decreasing the NaCl concentration, a stress equivalent to an increase of 0.48 MPa. Data from one cell are shown in Fig. 5. After the cell’s resting PD steadied at  $+9 \text{ mV}$  (65 min after impalement in ASW), hypotonic shock was imposed. The cell became rapidly more negative, although there was considerable variation in the membrane potential. When the PD stabilized at  $-15 \text{ mV}$  and the  $I$ - $V$  profile had achieved the typical hypotonic stress characteristics ( $I$ - $V$  1 in Fig. 5b, c, triangles;  $G_m^{\text{neg}} > G_m^{\text{pos}}$ ), DES was added. The cell rapidly became more negative, reaching a maximum negative PD of  $-55 \text{ mV}$  at 115 min. This was accompanied by a decrease in  $G_m^{\text{neg}}$  and an increase in  $G_m^{\text{pos}}$ , yielding a  $G$ - $V$  profile with

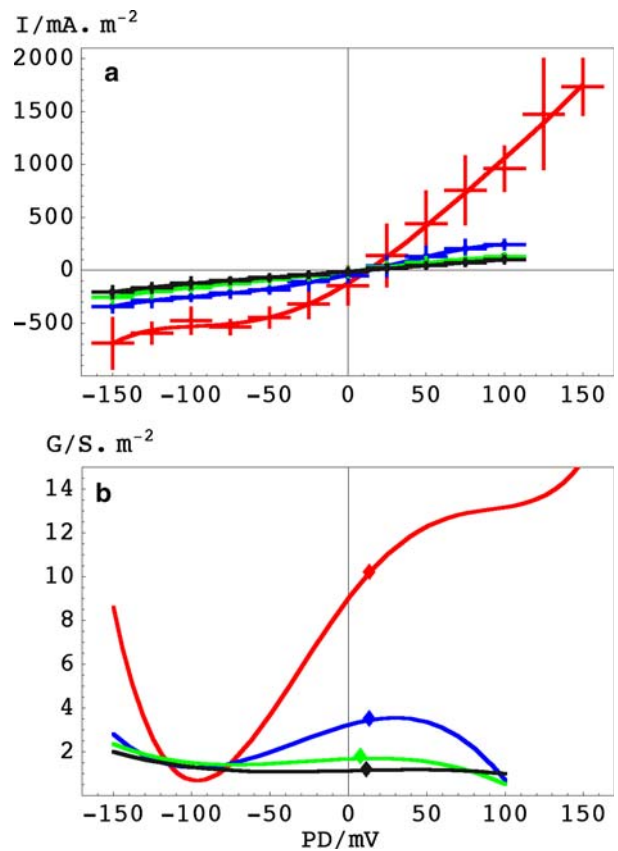
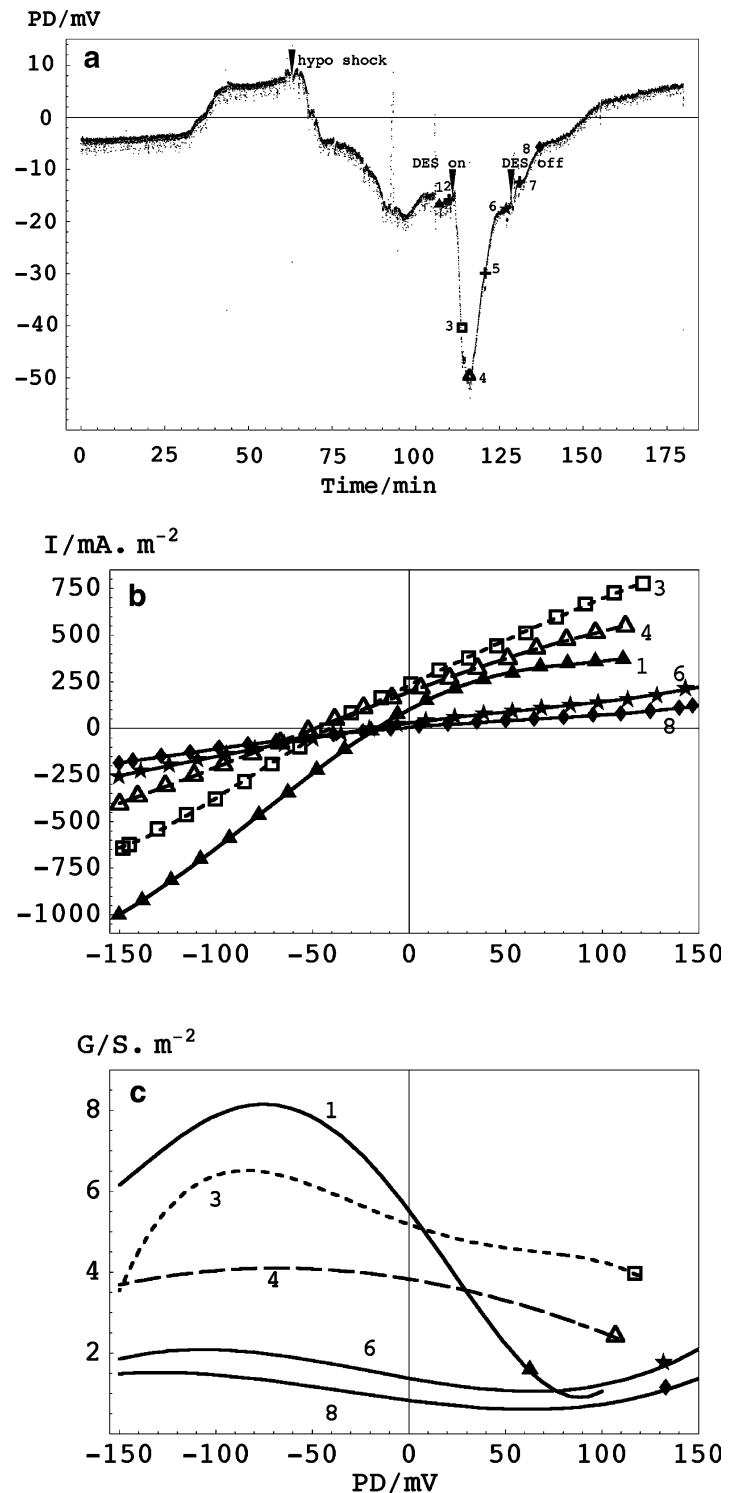


**Fig. 4** Statistics of inhibitor effects. **a**  $I$ - $V$  characteristics were collected into 25-mV bins (*horizontal bars*), and the standard error level was computed for each bin (*vertical lines*). *Red*: Control with light level at  $40 \mu\text{mol s}^{-1} \text{m}^{-2}$ , 14  $I$ - $V$  curves from five cells. Average conductance at resting PD of  $13.2 \text{ mV}$  was  $10.0 \text{ S m}^{-2}$ . *Blue*: Dim light at levels of  $0.23$ – $9.3 \mu\text{mol s}^{-1} \text{m}^{-2}$ , time in low light 29–50 min, seven  $I$ - $V$  curves from three cells. Conductance at resting PD of  $13.3 \text{ mV}$  was  $3.25 \text{ S m}^{-2}$ . *Green*: Effect of  $10 \mu\text{M}$  DCMU, control light levels, time of exposure 20–29 min, three  $I$ - $V$  curves from three cells. Average conductance at resting PD of  $7.6 \text{ mV}$  was  $1.5 \text{ S m}^{-2}$ . *Black*: Effect of  $10$ – $40 \mu\text{M}$  DES, control light, time of exposure 6–21 min, six  $I$ - $V$  curves from three cells. Average conductance at resting PD of  $11.5 \text{ mV}$  was  $1.1 \text{ S m}^{-2}$ . **b** Average  $G$ - $V$  profiles. *Diamond points* indicate resting membrane PD

$G_m^{\text{pos}} = G_m^{\text{neg}}$  and an overall low value, a profile consistent with a quiet, or inhibited, state (Fig. 5,  $I$ - $V$ s 3 and 4, empty squares and triangles). The PD recovered its more positive value by 130 min, but the  $G$ - $V$  profile did not resume the hypotonic stress profile, remained uniform across the PD range and continued to decrease (Fig. 5,  $I$ - $V$  6, stars). The washout of DES was accompanied by continued positive-going PD, but this was also true of control recovery from hypotonic stress (Bisson and Beilby 2002), so the effect cannot be attributed unambiguously to DES. Similar results were obtained with DCMU (results not shown): transient excursion to more negative PDs with decrease of  $G_m^{\text{neg}}$ . In this case some recovery of  $G_m^{\text{neg}}$  was observed upon DCMU washout.

**Fig. 5** Effect of 40  $\mu\text{M}$  DES at the time of hypotonic challenge, obtained by decreasing ASW osmotic pressure by 200  $\text{mOsmol kg}^{-1}$ . **a** Cell PD was data-logged at 1 point/s. The 2–3 mV scatter might represent an oscillation of the membrane PD, distorted by the data-logging rate. Larger scatter is observed at the time of solution change or  $I$ - $V$  curve measurement.

Downward arrowheads signify the beginning of the hypotonic challenge, the exposure and the washing out of DES. Times at which selected  $I$ - $V$  profiles were measured are indicated by a number and a symbol.  $I$ - $V$ s depicted by a cross are described but not shown as the diagram became too complex. The corresponding  $I$ - $V$ s in **b** use the same symbols as in **a**.  $I$ - $V$  profiles 1 (filled triangles) and 2 (not shown) were very similar, exhibiting stable hypotonic state.  $I$ - $V$  3 (empty squares and short dashed line in **b** and **c**) and  $I$ - $V$  4 (empty triangles and long dashed line in **b** and **c**) follow the transient effect of DES: increasingly negative reversal PD and decreasing conductance.  $I$ - $V$  5 (not shown) and  $I$ - $V$  6 (stars) are similar and indicate further conductance decrease.  $I$ - $V$  7 (not shown) and  $I$ - $V$  8 (filled diamond) show further conductance decrease despite the wash of DES. **c**  $G$ - $V$  profiles with the relevant symbols from **b** attached



### Turgor Measurement and Clamp

Before imposing the turgor clamp, turgor was measured at the time of  $I$ - $V$  data logging and as a function of external cell perfusion. We detected no changes in turgor at the time of voltage clamp to the bipolar staircase command. Turgor

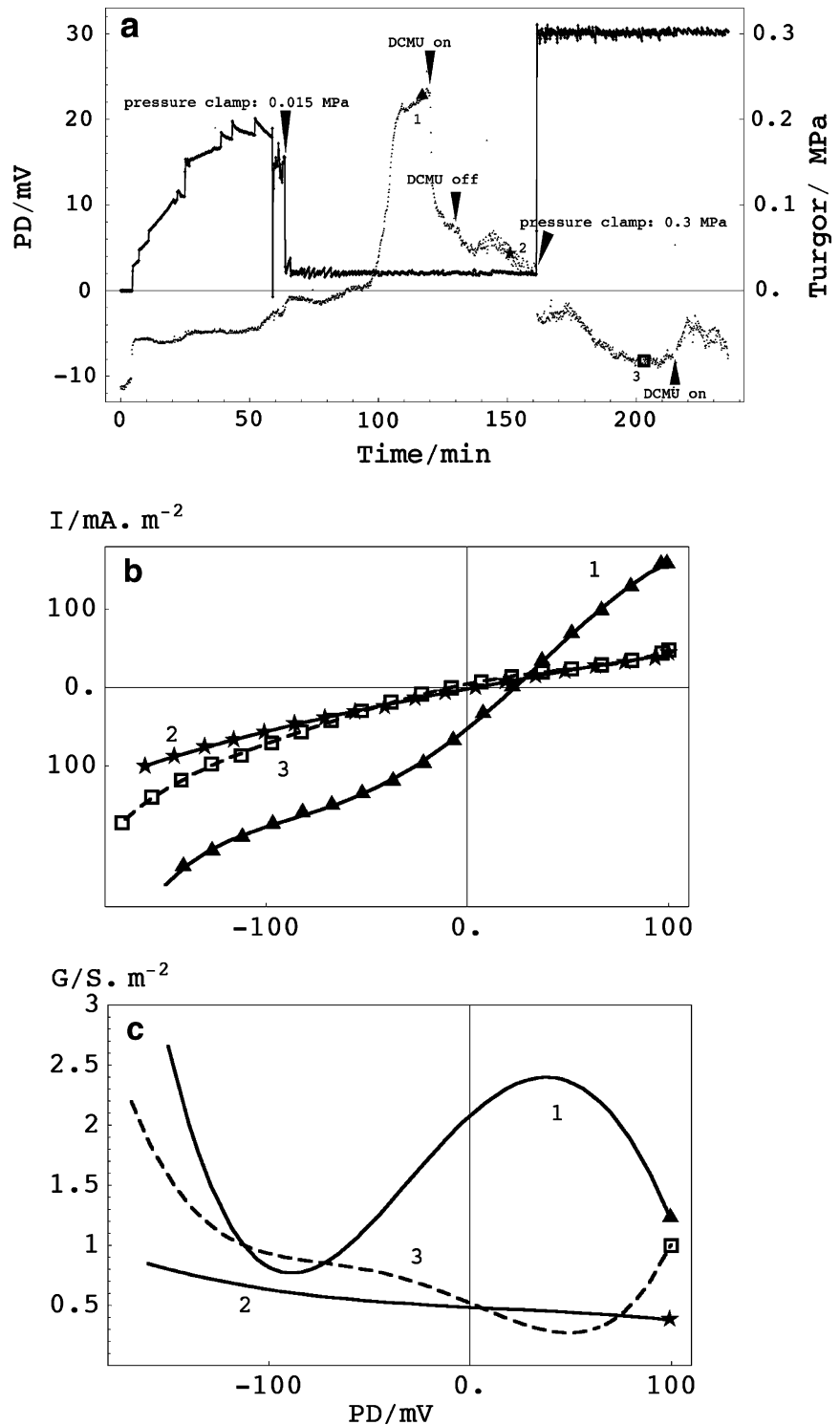
fell, however, if the cell was left in the small experimental chamber in a stagnant medium, probably due to evaporation. Consequently, we performed all our experiments while the media were flowing through the chamber.

The variability of the hypotonic state makes it difficult to assess what changes are caused by applied inhibitors.

One possible source of variability is turgor regulation; as the initially high turgor is regulated back toward its control value, regulatory responses will be modulated. We therefore employed the turgor clamp method (Wendler and Zimmermann 1982; Zhu and Boyer 1992; Heidecker et al. 2003), whereby cell sap volume is moved into or out of the cell to maintain turgor at a chosen level.

When turgor was reduced while maintaining the cell in control ASW by withdrawing cell sap from the vacuole, the response was similar to that seen when turgor was reduced by increasing external osmotic pressure (Fig. 6). This similarity of response supports the conclusion that the changes seen upon increasing external NaCl are due to osmotic effects and not chemical effects of the change in

**Fig. 6** The record of pressure (dark continuous line) and membrane PD (points) throughout an experiment (a), *I*-*V* profiles at selected times (b) and corresponding *G*-*V* profiles (c). Pressure was clamped to 0.015 MPa (first arrowhead) about 50 min after double impalement. When the resting PD increased to a steady level, *I*-*V* 1 (filled triangle) was recorded. Same symbol is used in b and attached to the *G*-*V* profile in c. DCMU 10 μM was applied at the second arrowhead. When resting PD reached a new steady state at a less positive value, DCMU was washed out (third arrowhead). *I*-*V* 2 (star) was recorded at minimum conductance. The pressure was then clamped to 0.3 MPa (tilted arrowhead). *I*-*V* 3 (empty square, dashed line in b and c) was recorded when the PD reached a new, more negative steady state. DCMU 10 μM was applied again at the inverted arrowhead



NaCl concentration. Figure 6 shows an experiment in which the cell was initially ( $t = 0\text{--}60$  min) maintained with free-running pressure. Some small variations occurred as the probe frequently clogged, and the meniscus was kept in the same position to maintain constant cell volume. This adjustment required occasional overcompensation of the piston placement (see “Materials and Methods”). At the time indicated by the first arrowhead, volume was withdrawn from the pipette to clamp the turgor to a lower value. Oscillations in the recorded pressure represent manual adjustments made to maintain the set turgor. These adjustments diminished over time as the cell acclimated to the pressure. After 40 min, the PD became much more positive (Fig. 6a) and the  $I\text{--}V$  curve exhibited the high  $G_m^{\text{pos}}$  typical of the accentuated pump state:  $I\text{--}V$  1, triangles (Fig. 6b, c). Table 1 shows the summary results for six cells clamped to low turgor, five stepped from 0.15 to 0 MPa and one stepped from 0.3 to 0.02 MPa. The time course of the response is similar to what was observed in doubly impaled cells (electrode + turgor probe) given an osmotic hypertonic challenge (Bisson and Beilby 2002), although those cells were more variable, reaching their new maximum PD in  $62 \pm 61$  min ( $n = 3$ ). Their maximum change in resting PD was significantly less than that of the clamped cells:  $+1.2 \pm 2.0$  compared to  $+22 \pm 3.9$  mV (see Table 1). The maximum change in PD may be greater in these experiments due to improved techniques in impalement (see “Materials and Methods”). However, turgor-clamped cells may also show a greater change in PD than unclamped cells because the turgor could not be regulated and, therefore, the regulatory response was exaggerated. All the turgor-clamped cells showed the typical “pump state”  $I\text{--}V$  curve, with  $G_m^{\text{pos}} > G_m^{\text{neg}}$ . The average  $I\text{--}V$  curve is shown in Fig. 7. Three of the six cells were maintained for 30–120 min at low turgor, and all cells maintained the typical high pump profile, with no variability in PD or  $I\text{--}V$  characteristics.

When turgor was increased by injecting sap into the vacuole, the response was again similar to that seen when turgor was increased by decreasing external osmotic pressure (Fig. 6), again consistent with the response to a decrease in external osmotic pressure being due to turgor pressure changes, not the change in NaCl concentration. Again, oscillations in the pressure trace represent repeated movements of the piston to achieve a constant pressure,

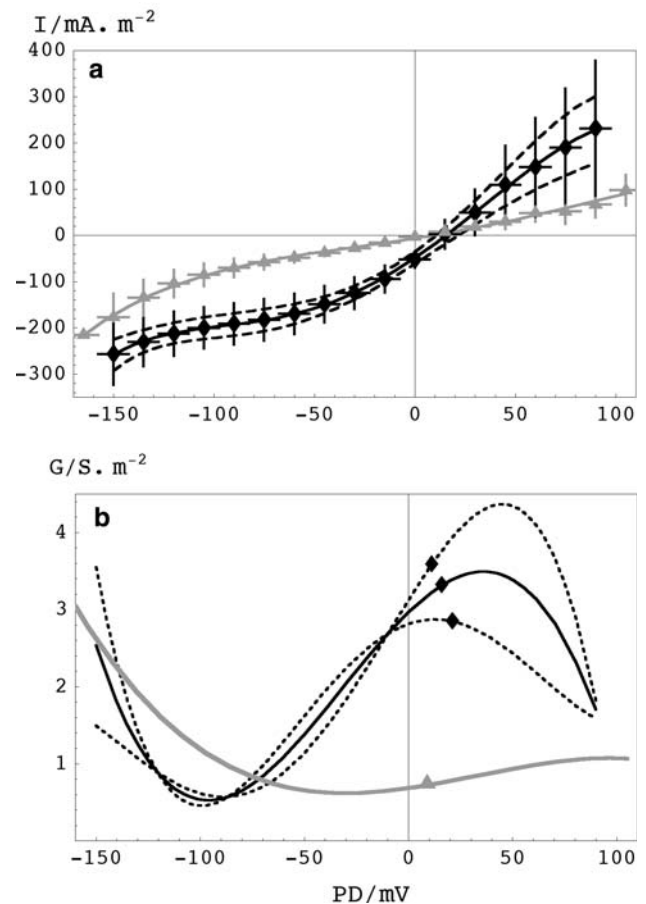


**Fig. 7** Statistics of low turgor clamp (a)  $I\text{--}V$  characteristics and (b)  $G\text{--}V$  characteristics; same line types in a and b. The maximal pumping state  $I\text{--}V$  characteristics (black filled diamonds) were collected after 1–2 h of low turgor clamp (12  $I\text{--}V$  curves from six cells). Data were gathered into 15-mV bins (dark horizontal bars) and the standard error was computed for each bin (dark vertical bars). A polynomial was fitted to the points (dark line). Large error bars indicate large variability in the currents in both positive and negative PD regions. To visualize the range of conductances, polynomials were fitted to points halfway through the error bars (dashed curves in both a and b). Inhibition by  $10 \mu\text{M}$  DCMU is shown by gray filled triangles, gray line and error bars (five  $I\text{--}V$ s from three cells) with exposure times of 10–20 min. The resting PDs for the average pump state  $I\text{--}V$  characteristics and those fitted at the half standard error are shown by dark filled diamonds in b. The average resting PD for the cells inhibited with DCMU is indicated by gray triangle in b

and the need for these movements decreased with time. The cell immediately became more negative, reaching a maximally negative value of  $-9$  mV in 45 min. The  $I\text{--}V$

**Table 1** Responses of turgor-clamped cells to alterations in turgor: data given as mean  $\pm$  SE ( $n$ )

Treatment	Turgor change (MPa)	Change in PD (mV)	Time to initiate change (min)	Time to maximal change (min)
Decreased turgor (hypertonic)	$-0.15 \pm 0.011$ (5)	$+22 \pm 3.9$ (5)	$26 \pm 4.7$ (5)	$68 \pm 18$ (5)
Decreased turgor (large step)	$-0.28$ (1)	$+10$ (1)	6 (1)	42 (1)
Increased turgor (hypotonic)	$0.27 \pm 0.011$ (5)	$-40 \pm 15$ (5)	$6.0 \pm 2.3$ (5)	$26 \pm 6.1$ (5)

profile shows  $G_m^{\text{neg}} > G_m^{\text{pos}}$ , as is typical for osmotically induced hypotonic stress (Fig. 6b, c, empty squares). The average of five cells exposed to increased turgor clamp is also shown in Table 1. Again, these results are comparable to those seen in doubly impaled cells experiencing osmotically induced hypotonic stress (Bisson and Beilby 2002), which began to change PD immediately and reached a maximum at  $28 \pm 5$  min. Also, the maximum change in PD was less:  $-7.3 \pm 4.8$  compared to  $-40 \pm 15$  mV in turgor-clamped cells (see Table 1). However, this maximal PD was not stable and typically became more positive with time. The maximal response  $I$ - $V$  curve with  $G_m^{\text{neg}} > G_m^{\text{pos}}$  was averaged in five turgor-clamped cells (dark line and error bars, Fig. 8a). The error bars indicate large variability in the conductance in both positive and negative PD regions. The conductance near the reversal PD was more reproducible. The gray line shows the average  $I$ - $V$  characteristics (four of five cells) 1 h after initiation of hypotonic stress. The data from the fifth cell were not included as the experiment was terminated 30 min after the pressure clamp. The  $G$ - $V$  curve (Fig. 8b) shows that after 1 h the conductance between  $-100$  and  $+100$  mV became more uniform. The diamonds and triangle in Fig. 8b indicate that the PD also shifted in the positive direction.

Rarely, cells show a slightly different time course (Fig. 9). Here, the rapid excursion to negative-going potentials after imposition of the pressure clamp (arrowhead) was accompanied by an increased conductance, uniform over positive and negative potentials (Fig. 9b, c, crosses). This state was short-lived and followed by a return to positive potentials and lower conductance, still uniform over positive and negative potentials. Such brief periods of high, uniform conductance were observed before in osmotically stressed cells (Beilby, unpublished results) and may represent a transient “emergency release” that sometimes accompanies hypotonic stress, proposed as a safety valve to prevent cell rupture under high turgor (Guggino and Gutknecht 1982). They are dissimilar to loss of seal around freshly impaled microelectrodes as such breaks typically take much longer to reseal. Some further oscillations were observed, but the high, uniform conductance did not recur.

#### Effect of Inhibitors on Turgor-Clamped Cells

Application of  $10 \mu\text{M}$  DCMU had a dramatic effect on the high-pump state characteristic of hypertonic stress (Fig. 6). The membrane PD fell from  $+23$  to  $+8$  mV in 23 min (Fig. 6a), while the  $I$ - $V$  curve showed a low and uniform conductance, characteristic of the quiet state ( $I$ - $V$  2, stars and  $G$ - $V$  2, Fig. 6b, c). For three cells, the average change in PD with DCMU was  $-13 \pm 3.0$  mV, requiring  $23 \pm 4.8$  min. Figure 7 shows the average  $I$ - $V$  curve for

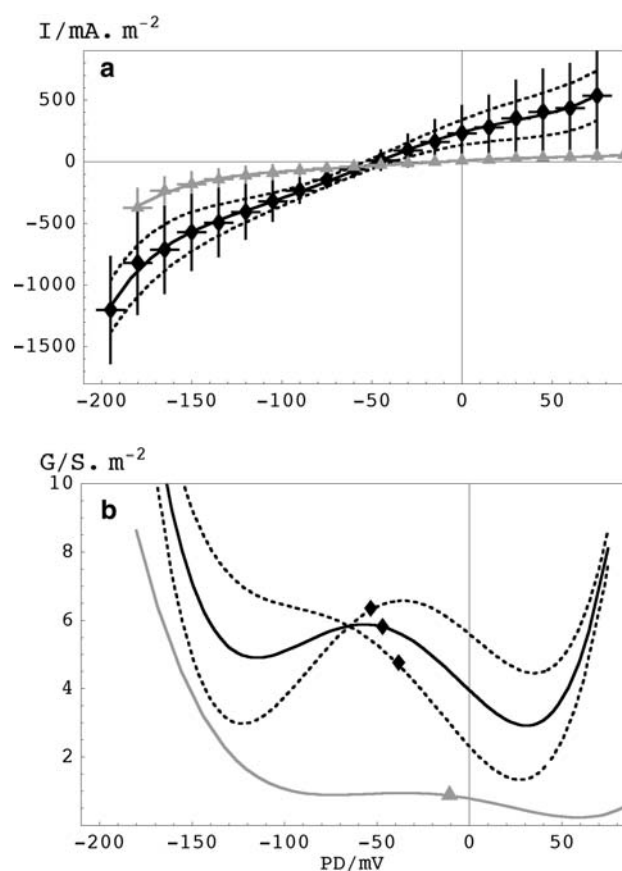
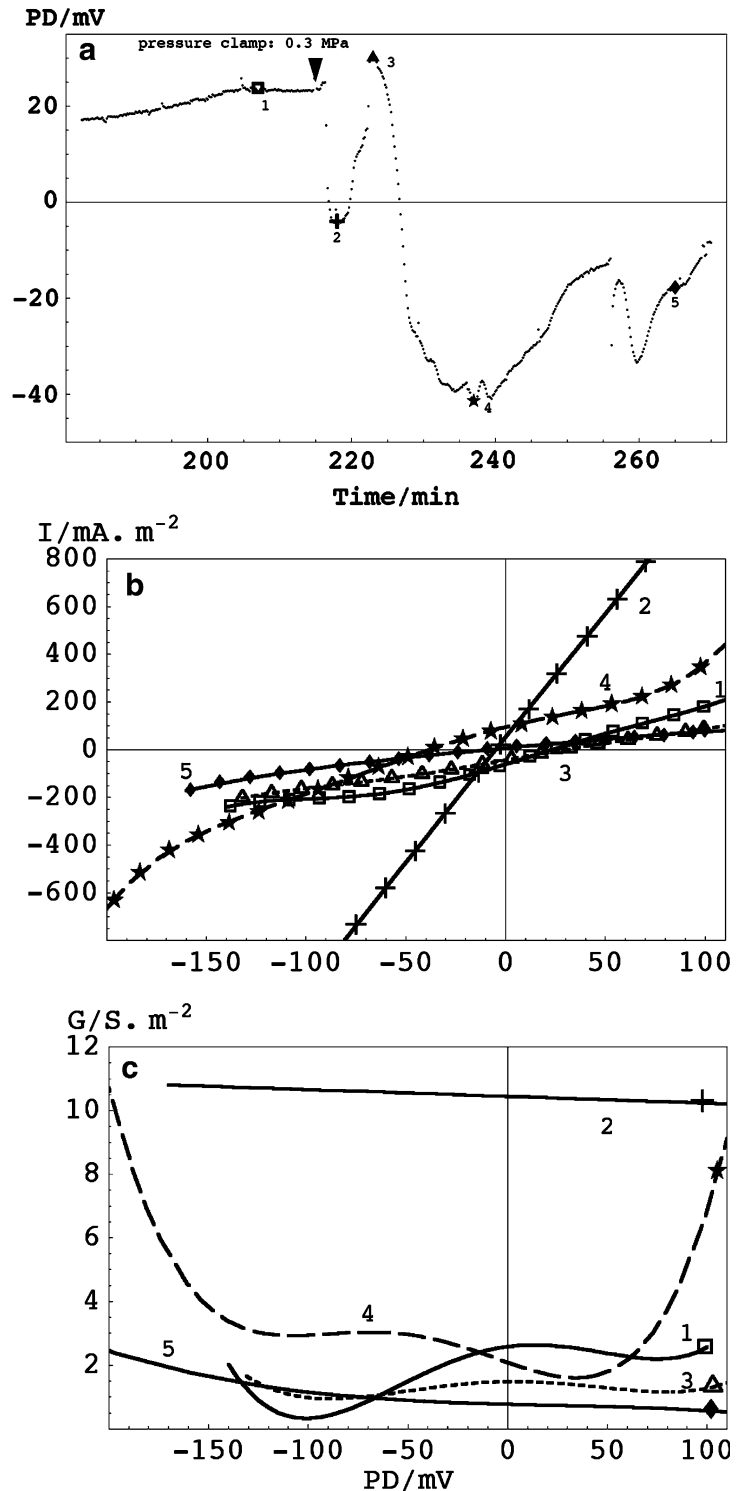


**Fig. 8** Statistics of high turgor pressure of 0.3 MPa (a)  $I$ - $V$  characteristics and (b)  $G$ - $V$  characteristics; same line types in a and b. The maximal response to hypotonic stress (dark diamonds) is shown in the average of eight  $I$ - $V$  curves from five cells. Data were collected into 15-mV bins (dark horizontal bars) and the standard error was computed for each bin (dark vertical bars). A polynomial was fitted to the points (dark line). Large error bars indicate large variability in the currents in both positive and negative PD regions. To visualize the range of conductances, polynomials were fitted to points half way through the error bars (dashed curves in a and b). The high conductance and negative PD of the hypotonic state spontaneously diminished after 1 h, despite the constant pressure. These data (four  $I$ - $V$ s from four cells) are treated in the same way as the maximal response and are shown as gray triangles and lines. The resting PDs for the average maximal response  $I$ - $V$  characteristics and those fitted at the half standard error are shown by dark filled diamonds in b. The average resting PD for the diminished response is indicated by gray triangle in b

the inhibited cells (gray line), with consistently low uniform conductance characteristic of the quiet state. In two out of three cells, recovery was complete with washout times of 28 and 23 min. The cell shown in Fig. 6 was monitored for only 15 min after DCMU washout before further manipulation and had insufficient time to recover.

When cells were clamped to high pressure and exhibited the usual negative membrane PDs, DCMU caused a positive excursion of the PD. In the cell shown in Fig. 6, the PD increased from  $-9$  to  $-4$  mV in 14 min. The average of

**Fig. 9** Response of one cell to a step increase in turgor. **a** Pressure clamp was changed from 0.015 to 0.3 MPa at *arrowhead*. recording times of *I-V* data are shown by numbers and symbols. *I-V* curve 1 (*empty squares*) was measured at 0.015 MPa. *I-V* 2 (*crosses*) was obtained after pressure clamp to 0.3 MPa while the resting PD exhibited a rapid swing to negative PD. *I-V* 3 (*empty triangles and short dashed line*) was recorded when the PD returned to a positive PD. *I-V* 4 (*stars and long dashed line*) was measured at the maximum negative PD, exhibiting the hypotonic state. *I-V* 5 (*filled diamonds*) was measured at the time of diminishing hypotonic state. **c** *G-V* characteristics with line types as in **b** and the relevant symbols attached



three cells exhibited an increase of  $12 \pm 4$  mV in  $23 \pm 4.8$  min. The *I-V* curves showed little immediate change upon inhibitor application. Since these changes are similar to those seen in noninhibited cells clamped to high turgor (Fig. 8), it is difficult to draw conclusions concerning the effect of the inhibitor.

## Discussion

### The Role of the $\text{K}^+$ Pump in Low Turgor Regulation

The  $\text{K}^+$  pump in *Ventricaria* and *Valonia* maintains the cell turgor in steady state, in a manner similar to the  $\text{H}^+$  pump in

charophytes and embryophytes (Beilby et al. 2006). Electrophysiologically, the  $I$ - $V$  profile under such conditions displays  $G_m^{\text{pos}} > G_m^{\text{neg}}$  and resting PD of about +20 mV (Beilby and Bisson 1999). Similar to the  $H^+$  pump, the electrophysiological signature of the  $K^+$  pump is inhibited by darkness and DCMU, presumably due to diminished ATP supply (Figs. 1–4). DES also inhibits this electrophysiological signature, and by analogy with its effect on  $H^+$  pumps (Keifer and Spanswick 1978; Scherer 1984), this may be a more direct effect. Under hypertonic stress (decreased turgor and increased medium salinity), the  $K^+$  pump is stimulated, as shown by electrophysiological and flux measurements (see Bisson et al. 2006, for a recent review). In the  $I$ - $V$  characteristics, this is seen as a transient increase in  $G_m^{\text{pos}}$ . The resultant increased uptake of  $K^+$  results in turgor regulation (Bisson and Beilby 2002). If the turgor is clamped to a low value, the pump is stimulated with a similar time course to hyperosmotic stress (see Table 1). In this case there is no change in salinity or  $K^+$  concentration in the medium. Thus, the stimulation is initiated by a pressure decrease alone. A similar activation on reducing turgor by addition of sorbitol in the external medium was observed in the  $H^+$  pump in the salt-tolerant charophyte *Lamprothamnium* (Al Khazaaly and Beilby 2007). In the present experiments we found that the  $K^+$  pump activity remains at a steady high level when the pressure is clamped at a low level. Five out of six pressure-clamped cells either showed no change in characteristics over 1–2 h of hypertonic stress or recovered completely from inhibition by DCMU. The sixth cell was not allowed to remain undisturbed long enough during DCMU washout to verify that it returned to the same PD and  $I$ - $V$  profile. These results imply that as long as pressure is low, the regulatory response is constant, suggesting a simple relationship between a turgor sensor and the activated transport system.

#### The Transporters in High Turgor Regulation

While it is clear that the response to hypertonic regulation requires active  $K^+$  transport to accumulate  $K^+$  in the vacuole in *Valonia* and *Ventricaria*, it remains unclear as to whether hypotonic regulation can occur purely by passive loss of  $K^+$  and  $Cl^-$  or whether an active step at either the plasma membrane or tonoplast is involved (see Bisson et al. 2006, for a recent survey). Anatomical observation of the interconversion of plasma membrane and tonoplast, particularly during aplanospore formation, led to the suggestion that the plasma membrane and the tonoplast are not distinct membranes but can share the same transporters (Shepherd et al. 2004). At the time of hypertonic regulation, the inward  $K^+$  pump at the inner membrane makes the membrane PD more positive and the membrane more conductive at positive PDs. At the time of hypotonic

regulation, the same pump could be transported to the outer membrane, pumping  $K^+$  out and making the membrane PD more negative and the membrane more conductive at negative PDs. In this case, we would predict that the pump-dominated steady, hypertonic and hypotonic states should all be sensitive to the same inhibitors. Alternatively, this apparent symmetry could be coincidental, and the hypotonic response could be due to a separate set of transporters, active or passive, which allow  $K^+$  and  $Cl^-$  to exit the cell to regulate turgor. We employed inhibitors of active transport to distinguish between these alternative models.

Earlier experiments had suggested a role for energy-dependent mechanisms for the hypotonic response. Bisson and Beilby (2002) exposed three cells at the time of hypo-osmotic regulation to brief period of 2 min of bright light ( $31.68 \mu\text{mol s}^{-1} \text{m}^{-2}$ ). The conductance increased and the PD became more negative (Fig. 6b and c in Bisson and Beilby 2002; note that the figure caption in that report erroneously describes the high-conductance  $I$ - $V$  profile as “light off”). The effect was reversible once the light was returned to the dim setting. This observation supported the hypothesis that there is an active element in the hypo-osmotic regulation, although it does not rule out the possibility that light acts as a signal that alters active or passive transport systems. In the experiments described here, we employed the inhibitors DCMU and DES to reduce the ambiguity. However, the results were unexpected. If there is an active outwardly directed  $K^+$  pump that makes the membrane potential more negative, we would expect that these inhibitors would make the membrane potential less negative. Instead, the hypo-osmotically stressed cells clearly respond to inhibitors by going more negative (Fig. 5a). This would be consistent with inhibition of the inwardly directed  $K^+$  pump, but the fact that the  $I$ - $V$  curve already displays a lower  $G_m^{\text{pos}}$  indicates that this pump is already inhibited. Moreover, this negative potential is accompanied by an increase in  $G_m^{\text{pos}}$ , which results in a high and relatively uniform conductance. This state is unlike other described states ( $I$ - $V$  and  $G$ - $V$  4, Fig. 5b, c). The negative-going PD suggests opening of  $K^+$  channels, but at the same time  $G_m^{\text{neg}}$  is dropping. When the membrane PD returns to preinhibitor level ( $I$ - $V$  and  $G$ - $V$  6 in Fig. 5b, c), the conductance becomes low and uniform as in the quiet state, yet the negative PD remains. This result suggests that there are several mechanisms keeping the membrane PD-negative. Thus, while the conductance decrease is consistent with outward  $K^+$  pump inhibition, the negative membrane PD is not.

We again used the pressure clamp to distinguish the pressure and osmotic effects. The hypotonic state was initiated by high pressure. However, the response was variable despite the constant high turgor (Figs. 6, 8, 9). The

oscillations observed in the cell depicted in Fig. 9 suggest the existence of a feedback mechanism, but the parameters involved are unlikely to arise from the turgor sensor signal. All cells, if pressure-clamped for a sufficiently long time, exhibited positive-going membrane PD and diminishing conductance (Figs. 6, 8, 9) with a time course similar to that observed in osmotically stressed, turgor-regulating cells (see Table 1). The turgor-clamped cells did not display the transient negative change in membrane PD and conductance decrease upon exposure to DCMU. Possible DCMU-induced changes in PD were small and positive-going—too difficult to distinguish from the trend shown by uninhibited cells (Fig. 8).

What is the difference between osmotically stressed and turgor-clamped cells? One possibility is that in cells that are osmotically stressed by diluting seawater, the decrease in  $K^+$  concentrations, although slight, has a significant effect. We previously showed (Beilby and Bisson 1999) that the increase in  $[K^+]_o$  decreased membrane conductance while decreases in  $[K^+]_o$  increased membrane conductance. This is the opposite of what would be expected if  $K^+$  conductance dominated the overall membrane conductance. However, these changes were slow and accompanied by oscillations (Beilby and Bisson 1999), and we proposed that some feedback mechanism responded to alterations in  $K^+$  availability by altering transport. Moreover, the  $I$ - $V$  profile of cells in low  $[K^+]_o$  is similar to that observed in hypotonically stressed cells. This is difficult to explain since hypotonically stressed cells lose KCl to regulate their turgor, while presumably cells in low  $[K^+]_o$  need to transport in more  $K^+$ . We suggest that the hypotonic-like state seen at low  $K^+$  might represent changes in  $K^+$  transport at the tonoplast, replenishing  $K^+$  lost from the cytoplasm from the high concentration in the vacuole (Gutknecht 1966). Future experiments are being designed to study the influence of cytoplasmic  $K^+$  concentration on the transport parameters.

If  $K^+$  permeability at the outer membrane is playing a significant role in generating the negative membrane PD at the time of high turgor regulation,  $K^+$ -channel blockers should decrease  $G_m^{neg}$  and make membrane PD more positive. However, the application of 20 mM tetraethylammonium chloride (TEA, an inhibitor of many types of  $K^+$  channels) to the outside of the cell had no effect on the hypotonic  $I$ - $V$  characteristics (data not shown). If there is a channel-mediated  $K^+$  outflow, the channel is not TEA-sensitive.

Other putative channel blockers have been studied. Heidecker et al. (2003) employed  $Ba^{2+}$  as a  $K^+$  channel inhibitor and DIDS as a  $Cl^-$  channel inhibitor.  $Ba^{2+}$  decreased membrane conductance, as would be predicted for a channel inhibitor. However, the authors used an unusual technique of measuring voltage relaxation

following a high, brief voltage pulse, which gives values of conductance much higher than those obtained by other methods (see Bisson et al. 2006, for a review). They showed little change in membrane potential, with a slight negative tendency. Since the equilibrium potential across the plasma membrane is negative, one would predict that inhibiting  $G_K$  would shift the membrane potential positive. They also found that  $Ba^{2+}$  inhibited hypertonic, but not hypotonic, regulation. The hypertonic response probably requires passive  $K^+$  uptake across the plasma membrane to provide substrate for the active accumulation at the tonoplast. However, the lack of involvement of passive  $K^+$  loss at the plasma membrane is unexpected, although it is possible that an inwardly rectifying,  $Ba^{2+}$ -sensitive  $K^+$  channel is responsible for uptake during hypertonic regulation and a different outwardly rectifying,  $Ba^{2+}$ -insensitive channel is responsible for loss during hypotonic regulation. They also showed that DIDS, a putative  $Cl^-$  channel blocker, inhibited hypertonic but not hypotonic regulation.

More recently, Binder et al. (2006) utilized the permeant inhibitor 5-nitro-2-(3-phenylpropylamino) benzoic acid (NPPB), a putative anion channel blocker. They showed that it caused the membrane potential to go more positive while conductance decreased, as would be expected if it were blocking either  $Cl^-$  or  $K^+$  channels at the plasma membrane. Hypotonic regulation was inhibited but at high concentrations that could cause nonspecific effects. Nonetheless, these results are compatible with a strong role for channel activity in hypotonic regulation.

In summary, we have shown that imposing turgor stress by the turgor clamp yields electrophysiological responses that are similar to those evoked by equivalent osmotic stresses but more intense and longer-lasting. The hypotonic regulatory response is also stronger under turgor clamp but still transient and exhibits oscillatory responses. To ascertain whether similar transport systems were involved in the hypo- and hypertonic regulatory responses, we examined whether conditions that inhibited the hypertonic response also inhibited the hypotonic response. Conditions that alter the availability of energy sources (darkness, the photosynthetic inhibitor DCMU) and the active transport inhibitor (DES) inhibit the hypertonic response, but the sensitivity of the hypotonic response is more difficult to assess because of its inherent variability. However, osmotically stressed cells show a large, transient, negative excursion of PD during hypotonic stress, the clearest counterindication to the hypothesis of the symmetry of low and high turgor regulation.

**Acknowledgments** We thank Professor John Morley (School of Medical Science, Physiology and Pharmacology, Vision and Cognition Laboratory, University of New South Wales) for making his

bevelled available to us for pressure probe microelectrode tip preparation. The research was partly supported by a Faculty Research Grant on turgor pressure sensing and transduction (to M. J. B.).

## References

- Al Khazaaly S, Beilby MJ (2007) Modelling ion transporters at the time of hypertonic regulation in *Lamprothamnium succinctum* (Characeae, Charophyceae). *Charophytes* 1:28–47
- Beilby MJ (1990) Current-voltage curves for plant membrane studies: a critical analysis of the method. *J Exp Bot* 41:165–182
- Beilby MJ, Bisson MA (1999) Transport systems of *Ventricaria ventricosa*: *I/V* analysis of both membranes in series as a function of  $[K_0^+]$ . *J Membr Biol* 171:63–73
- Beilby MJ, Bisson MA, Shepherd VA (2006) The electrophysiology of turgor regulation in charophyte cells. In: Volkov AG (ed) *Plant electrophysiology—theory and methods*. Elsevier, New York, pp 375–406
- Binder KA, Heisler F, Westhoff M, Wegner LH, Zimmermann U (2006) Elucidation of the mechanisms underlying hypo-osmotically induced turgor pressure regulation in the marine alga *valonia utricularis*. *J Membr Biol* 213:47–63
- Bisson MA, Beilby MJ (2002) The transport systems of *Ventricaria ventricosa*: II. Hypotonic and hypertonic turgor regulation. *J Membr Biol* 190:43–56
- Bisson MA, Beilby MJ, Shepherd VA (2006) Electrophysiology of turgor regulation in marine siphonous green algae. *J Membr Biol* 211:1–14
- Damon EB (1930) Dissimilarity of inner and outer protoplasmic surfaces in *Valonia*. *J Gen Physiol* 13:207–221
- Davis RF (1981) Electrical properties of the plasmalemma and tonoplast in *Valonia ventricosa*. *Plant Physiol* 67:825–831
- Guggino S, Gutknecht J (1982) Turgor regulation in *Valonia macrophysa* following acute osmotic shock. *J Membr Biol* 67:155–164
- Gutknecht J (1966) Sodium, potassium and chloride transport and membrane potentials in *Valonia ventricosa*. *Biol Bull* 130:331–344
- Heidecker M, Wegner LH, Binder K-A, Zimmermann U (2003) Turgor pressure changes trigger characteristic changes in the electrical conductance of the tonoplast and the plasmalemma of the marine alga *Valonia utricularis*. *Plant Cell Environ* 26:1035–1051
- Keifer DW, Spanswick RM (1978) Activity of the electrogenic pump in *Chara corallina* as inferred from measurements of the membrane potential, conductance, and potassium permeability. *Plant Physiol* 62:653–661
- Kopak MJ (1933) *Physiological studies on Valonia ventricosa*. *Carnegie Inst Wash Year Book* 32:273–275
- Osterhout WJV (1924) On the importance of maintaining certain differences between cell sap and external medium. *J Gen Physiol* 7:561–564
- Scherer GFE (1984) Subcellular localization of  $H^+$ -ATPase from pumpkin hypocotyls (*Cucurbita maxima* L.) by membrane fractionation. *Planta* 160:348–356
- Shepherd VA, Beilby MJ, Bisson MA (2004) When is a cell not a cell? A theory relating coenocytic structure to the unusual electrophysiology of *Ventricaria ventricosa* (*Valonia ventricosa*). *Protoplasma* 223:79–91
- Wendler S, Zimmermann U (1982) A new method for the determination of hydraulic conductivity and cell volume of plant cells by pressure change. *Plant Physiol* 69:990–1003
- Zhu GL, Boyer JS (1992) Enlargement in *Chara* studied with a turgor clamp: growth rate is not determined by turgor. *Plant Physiol* 100:2071–2080